Soft Matter

REVIEW

View Article Online
View Journal | View Issue

Cite this: *Soft Matter*, 2015, **11**, 222

Smectite clay – inorganic nanoparticle mixed suspensions: phase behaviour and rheology†

Louise Bailey,*[a] Henk N. W. Lekkerkerker[b] and Geoffrey C. Maitland[c]

Smectite clay minerals and their suspensions have long been of both great scientific and applications interest and continue to display a remarkable range of new and interesting behaviour. Recently there has been an increasing interest in the properties of mixed suspensions of such clays with nanoparticles of different size, shape and charge. This review aims to summarize the current status of research in this area focusing on phase behaviour and rheological properties. We will emphasize the rich range of data that has emerged for these systems and the challenges they present for future investigations. The review starts with a brief overview of the behaviour and current understanding of pure smectite clays and their suspensions. We then cover the work on smectite clay-inorganic nanoparticle mixed suspensions according to the shape and charge of the nanoparticles – spheres, rods and plates either positively or negatively charged. We conclude with a summary of the overarching trends that emerge from these studies and indicate where gaps in our understanding need further research for better understanding the underlying chemistry and physics.

Received 2nd August 2014
Accepted 20th November 2014

DOI: 10.1039/c4sm01717j

www.rsc.org/softmatter

Introduction

Smectite clay minerals are used in a wide range of industrial applications,[1–3] from absorbents[4] to drilling fluids[5] and nanocomposites,[6] and at the same time present significant scientific challenges.

The remarkable range of their functionality arises from the subtleties of the crystal chemical composition[7–13] and colloid chemistry[14–16] which drive the interaction of the clay particles to build sols, gels, glasses, and even liquid crystals.[17–22]

[a]*Schlumberger Gould Research, High Cross, Madingley Road, Cambridge, CB3 0EL, UK. E-mail: bailey7@slb.com*

[b]*Van 't Hoff Laboratory for Physical and Colloid Chemistry, Utrecht University, Padualaan 8, 3584 CH Utrecht, The Netherlands*

[c]*Department of Chemical Engineering, Imperial College London, South Kensington, London, SW7 2AZ, UK*

† Electronic supplementary information (ESI) available. See DOI: 10.1039/c4sm01717j

Louise Bailey is a Principal Research Scientist in the Drilling Technologies group at Schlumberger Gould Research in Cambridge, UK. A colloid scientist and rheologist, since joining Schlumberger in 1990 she has worked on drilling fluids and their interactions with rock formations as part of the drilling process.

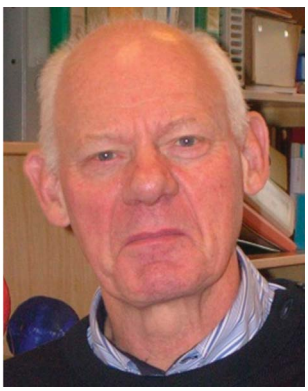

Henk Lekkerkerker is an Emeritus Professor in Physical Chemistry at Utrecht University and a Visiting Professor in the Department of Chemical Engineering of Imperial College London. His primary area of research is the phase behaviour, including long-lived metastable and non-equilibrium states, of colloidal suspensions of particles with different shapes, sizes and interactions. Together with Remco Tuinier he wrote the book Colloids and the Depletion Interaction (Springer, Heidelberg, 2011). He enjoys bicycling in the countryside in the Netherlands but also likes the challenge the Mont Ventoux presents.

Further richness (complexity) comes from the drive for optimisation of properties such as rheology by modifying the particle interactions through the addition of salts, polymers and, more recently, other colloidal particles. The effects of polymers and salt have been widely studied and reviewed;[15,19,23,24] in this review we focus on the effects of added nanoparticles, notably on the rheology and phase behaviour.

We first review recent developments with smectite clays (physical chemistry, rheology and phase behaviour) to give the necessary background, before focusing on the effects of adding nanoparticles of different shape, size and charge, such as inorganic oxides, mixed-metal hydroxides and other clays. In conclusion we summarise the overarching trends that emerge from these studies and indicate where gaps in our understanding need further research for better defining the underlying chemistry and physics. In addition, we give representative TEM images of the smectite clays and inorganic nanoparticles in the ESI.†

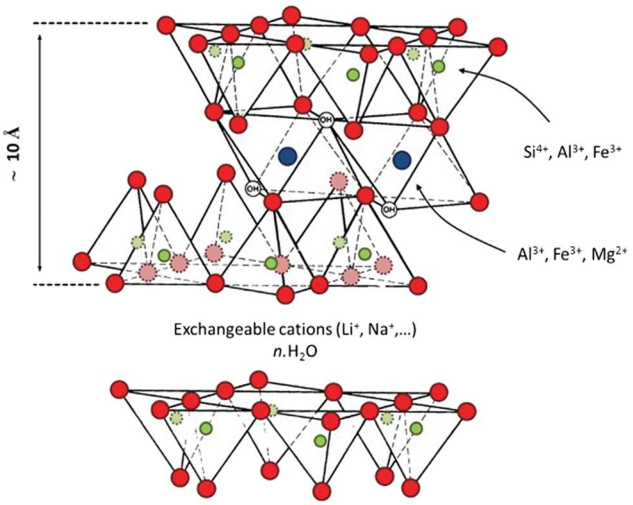

Fig. 1 Crystal structure of a dioctahedral smectite nanosheet (reproduced with permission from Paineau *et al.*,[27] after Grim[28]).

Smectite clays

Smectite clay minerals, their structure

Smectites are phyllosilicate minerals[7,25] characterized by a 2 : 1 layer structure in which two tetrahedral silica sheets either side of an octahedral sheet sharing apical oxygens (see Fig. 1). Hectorite is a trioctahedral smectite with a brucite octahedral layer, montmorillonite and beidellite are dioctahedral smectites with a gibbsite octahedral layer, and in nontronite the octahedral sheet is predominantly iron hydroxide. In addition to the naturally occurring smectites, smectite minerals can be synthesised.[10,26] Particularly well studied is Laponite RD, a synthetic hectorite. Closely related, but with significantly different properties, is Laponite B a fluoro-hectorite in which fluorine ions replace hydroxyl groups in the octahedral layers.[18,26] Smectites have a layer charge between 0.2e and 0.6e per half unit cell (corresponding to a surface charge ranging from -0.07 to -0.21 C m^{-2}) arising from isomorphic substitutions in the octahedral or tetrahedral sheets. In hectorite, the substitution is of Mg^{2+} by Li^{+} in the octahedral sheet. In the dioctahedral minerals both tetrahedral and octahedral substitutions occur; in montmorillonite the octahedral substitutions dominate (Mg^{2+} for Al^{3+}) whereas in beidellite and nontronite the charge arises predominantly from substitutions in the tetrahedral sheet (Al^{3+} and Fe^{3+} for Si^{+4}). A comparison of the distribution of charge locations for a range of smectite clays is shown in Fig. 2. These variations lead to quite different phase behaviour[27] with some smectites forming liquid crystal phases and others only gels.

As well as the permanent negative charges due to isomorphic substitutions in the clay layers, pH dependent charges develop on the surface hydroxyl groups. This can lead to positive charges on the edges. The extent to which these edge charges can be

Geoffrey Maitland is Professor of Energy Engineering at Imperial College London and President of the Institution of Chemical Engineers for 2014–15. He has had 20 years' experience of oil and gas R&D with Schlumberger and has a continuing interest in developing smart fluid and soft solid materials for oilfield applications. His research interests involve relating molecular and colloidal interactions to bulk fluid properties with applications in carbon capture and storage and cleaner, more efficient production and use of hydrocarbons, including shale gas and gas hydrates.

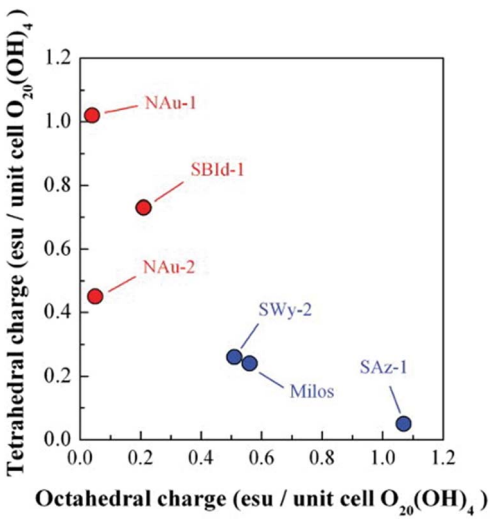

Fig. 2 Comparison of the charge location (tetrahedral *versus* octahedral) for different smectite clays: nontronites: NAu-1 and NAu-2 (Australia); beidellite: SBId-1 (Idaho, USA); montmorillonites: SWy-2 (Wyoming, USA), SAz-1 (Arizona, USA), Milos (Greece). Reproduced with permission from Paineau *et al.*[27]

accessed depends on the degree of surface charge and the ionic strength of the suspending medium.[26,29–34] The electrical double layer around smectite clay platelets is shown schematically in Fig. 3, which includes the effect of pH and indifferent electrolyte concentration on the sign and distribution of these edge charges. The combination of the variation in isomorphic substitution and edge charge heterogeneity leads to further richness in smectite clay behaviour.

Smectites are known as the swelling clays due to their behaviour on hydration; here the hydration energy of interlayer cations can overcome the attractive forces between the cations and the charged clay layers, allowing water to enter the interlayer region and swell the system.[25] This has been the subject of a vast and fascinating literature.[35–60] However, rheology and phase studies mostly deal with low concentrations of the homoionic Na exchanged clays which dissociate into individual sheets of thickness ~1 nm with fully developed double layers. A key issue in understanding all these phenomena is knowledge of the inter-particle forces and how they change with clay type, counter cation, pH and electrolyte concentration. DLVO theory quantifying double layer interactions has played a major role here,[14,17,61] although there has been much debate concerning other possible contributions to the clay interactions[62–64] especially long range attraction between like charged particles[65–67] and these issues are not fully resolved at present.[68,69]

The shapes of smectite clay particles vary from plate-like (montmorillonite, beidellite) to lath-like (hectorite, nontronite) and they are highly polydisperse. Smectite clay particles range in size from 0.1–2 μm (except for the synthetic Laponites which are much smaller, with diameters about 25–40 nm). Fig. 4 shows the structure and dimensions of a typical montmorillonite platelet aggregate, illustrating the high aspect ratio and flexibility of these clay platelets.

Sol–gel transitions

Smectite clays form gels at volume fractions as low as 1 vol%, a feature that has been studied for a long time.[71–77] It was suggested by Van Olphen[78,79] that the gel was formed by the attraction between the edges and the faces of the clay platelets. This interpretation of the gel structure is referred to as the house of cards structure. Norrish[61] suggested that the repulsive

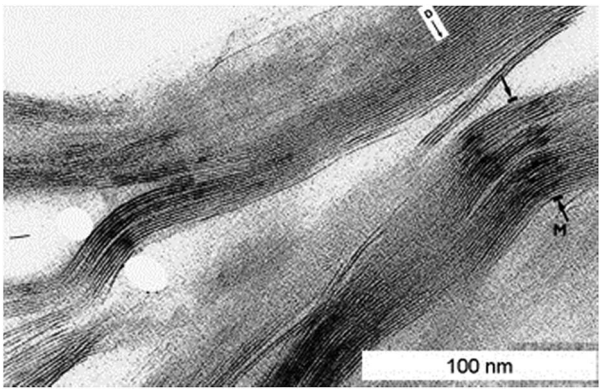

Fig. 4 TEM image of a purified natural montmorillonite dispersed in water. Reproduced from Pellenq and Van Damme.[70]

force caused by interacting double layers was responsible for the gel structure. There have been significant developments in the ability to study the structure of clay dispersions using techniques such as cryo-TEM,[80] ultra small angle X-ray scattering,[81] X-ray fluorescence microscopy,[82] environmental scanning electron microscopy,[83] transmission X-ray microscopy,[84–86] and differential interference contrast microscopy.[87] This has led to some convergence of the views on the structure of clay gels. It appears that the house of cards structure is limited to the regime of low pH and moderate to high electrolyte concentration where the positive edge charge is not screened by the extent of the double layer from the large negative face charge.[26,29,30] The change in microstructure as electrolyte concentration is increased is illustrated in Fig. 5.

The sol–gel state diagram for Wyoming and Turkey montmorillonites was mapped out by Abend and Lagaly[19] for ionic strengths ranging from 10^{-5} to 1 M, and up to 5 wt% clay, (at unspecified pH, probably ~7) – see Fig. 6. At low electrolyte

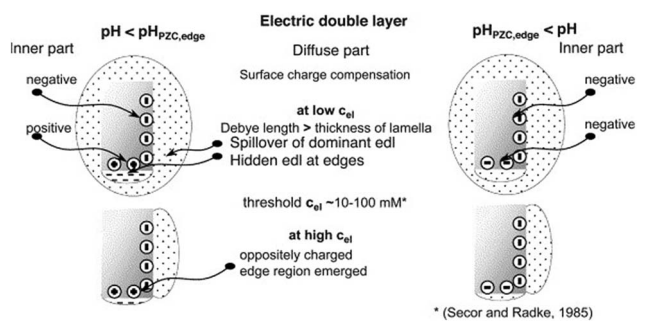

Fig. 3 Schematic representation of the electrical double layers (edl) around montmorillonite platelets under different solution conditions, reproduced from Tombácz and Szekeres[30] after Secor & Radke.[29]

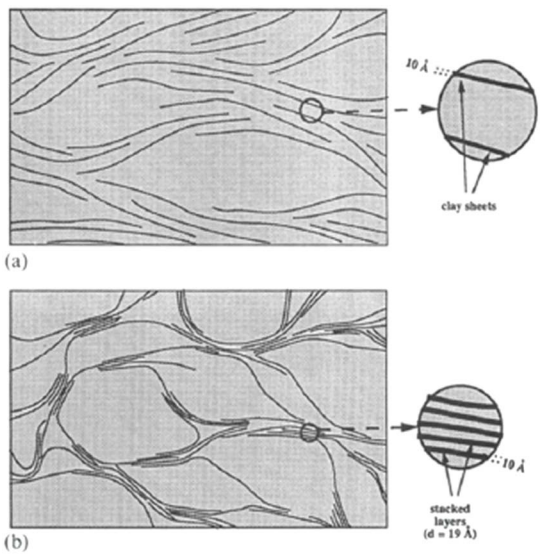

Fig. 5 Schematic representation of the structure of smectite gel (a) dispersed in fresh water and (b) effect on the structure of addition of salt. Reproduced from Morvan *et al.*[81]

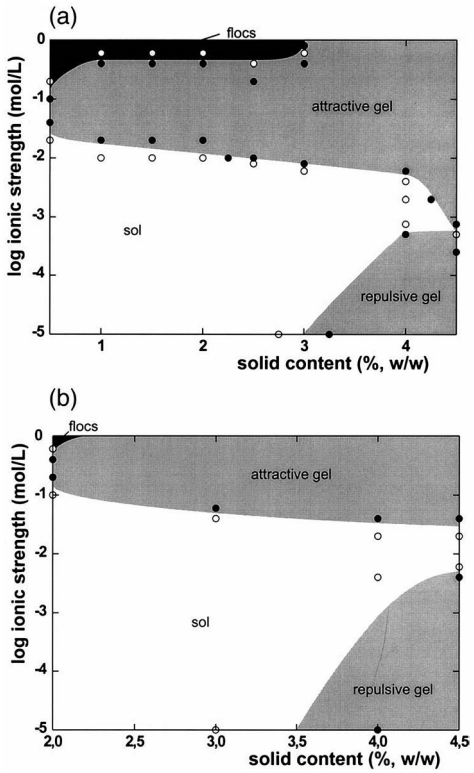

Fig. 6 Sol–gel state diagrams for two sodium montmorillonites and NaCl. (a) Turkey M50, (b) Wyoming M40A. Reproduced from Abend & Lagaly.[19]

concentrations repulsion dominates giving rise to a repulsive gel, or in modern terminology a Wigner glass, while at high electrolyte concentration (0.1 M and above) an attractive gel is observed. The sol-repulsive gel boundary was ~3.5 wt% at low electrolyte concentrations, rising to 4.5 wt% at intermediate ionic strengths. It can be seen from Fig. 6, that while Wyoming and Turkey montmorillonites differ only slightly in their absolute layer charge, 0.28 *vs.* 0.33 eq. per unit, (and in the way this is distributed between the octahedral and tetrahedral layers) yet, whilst the qualitative features of their sol–gel diagrams are similar, there are marked quantitative differences between the regions where the flocs, and the attractive and repulsive gels, are observed. Similar variations in the state diagrams for different montmorillonites have been observed in a number of other studies which also indicate the importance of particle size, shape, and aspect ratio. Michot *et al.*[88] and Bailey *et al.*[89] found a sol–gel transition for Wyoming montmorillonite at low ionic strength at ~1.5–2.5 wt%, the sol–gel transition increasing with particle size and anisotropy.[88] Vali and Bachman[80] report a slightly higher transition at 3 wt% for Nevada montmorillonite. Ten Brinke *et al.*[90] found the sol–gel transition for hectorite was lower at ~1.5 wt%. Mourchid *et al.*[91–94] and other workers[22,95,96] found very similar state diagrams for Laponite RD, with the sol–repulsive gel transition at ~0.5 wt%. In all these cases the gel transition occurs at a concentration at which the effective hydrodynamic volumes of the particles, extended by the range of the electrical double layer, begin to overlap.

Clay liquid crystals

Unlike other plate-like colloids, there was until recently little evidence to show smectite clays displayed Onsager type isotropic (I)/nematic (N) phase transitions. Langmuir[77] had observed I/N phase separation in a hectorite suspension after several hundred hours at coexisting concentrations 2.0–2.2 wt%. However subsequent workers could not reproduce this observation. In fact in a footnote (p 877) in his original paper[77] Langmuir had mentioned that the phase separation was non-reproducible.

In 1996 Gabriel *et al.*[18] observed nematic liquid crystal textures in aqueous gels of montmorillonite and of Laponite B (a synthetic fluoro-hectorite). They occasionally observed samples of Laponite B which showed both the isotropic and nematic phases separated by a sharp border. However, as in Langmuir's experiments, the observation was not reproducible. The state diagrams obtained are illustrated in Fig. 7. The nematic gel was also observed by Lécolier[93,97] in Laponite RD suspensions.

Fossum and co-workers[98–100] observed the I/N phase transition in suspensions of Na fluoro-hectorite synthetic clay. Miyamoto *et al.*[101] also observed isotropic and nematic liquid

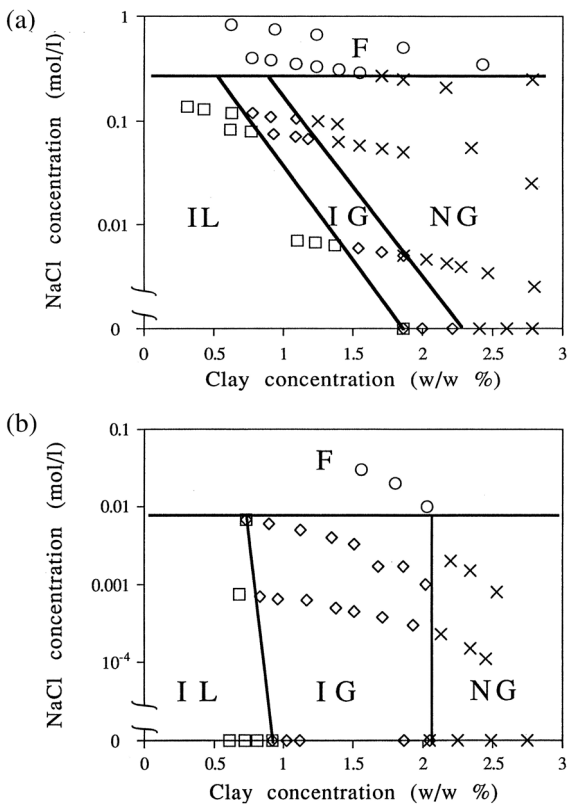

Fig. 7 (a) State diagram of the bentonite suspensions *versus* clay and NaCl concentrations. (○, F) Flocculated; (□, IL) isotropic liquid; (◇, IG) isotropic gel; (×, NG) nematic gel. (b) Phase diagram of the Laponite suspensions *versus* clay and NaCl concentrations. (○, F) Flocculated; (□, IL) isotropic liquid; (◇, IG) isotropic gel; (×, NG) nematic gel. Reproduced with permission from Gabriel *et al.*,[18] Copyright 1996 American Chemical Society.

crystal phases in suspensions of a different fluoro-hectorite. The key difference between these fluoro-hectorites and Laponite B is their much larger particle size (~0.1–3 μm *vs.* 30–40 nm). The first unambiguous observations of I/N phase transitions in natural smectite clays came with the work of Michot and co-workers on nontronite[21,102] and beidellite.[103] In both cases these are smectites with predominantly tetrahedral substitutions (see Fig. 2). The state diagram for nontronite clay suspensions is given in Fig. 8 and the observation of the nematic phase and its increase in phase volume with increasing clay concentration in Fig. 9.

It is interesting that for the pure clays montmorillonite, hectorite, nontronite and beidellite, even though their shape gives them the propensity to form liquid crystalline domains,[104,105] their suspension behaviour is quite different. With montmorillonite and hectorite, gel formation pre-empts the formation of ordered phases, whereas for beidellite and nontronite liquid crystalline phases are readily observed. It seems, therefore, that generally (though not exclusively, because fluorinated hectorite forms ordered phases) clays with charges located in the outer tetrahedral silicate layers proceed to form liquid crystalline phases whereas for those where the charge resides in the inner octahedral layer, gelation intervenes. However, the underlying physics behind this observation is not currently understood. Some insight into this behaviour may be gained from the work of Bleam[106] who investigated the importance of charge localization on the electrostatic potentials and found that the electrostatic potential curves of beidellite show considerably more pronounced maxima and minima compared to montmorillonite. However, the precise way in which these subtle changes in interaction potential result in such different behaviour has yet to be resolved. The recent simulations of Delhorme *et al.*[107] suggest that the edge/face charge heterogeneity plays a significant role in determining gel, glass and I/N states. A high charge heterogeneity leads to a suppression of the I/N transition in favour of a gel phase.

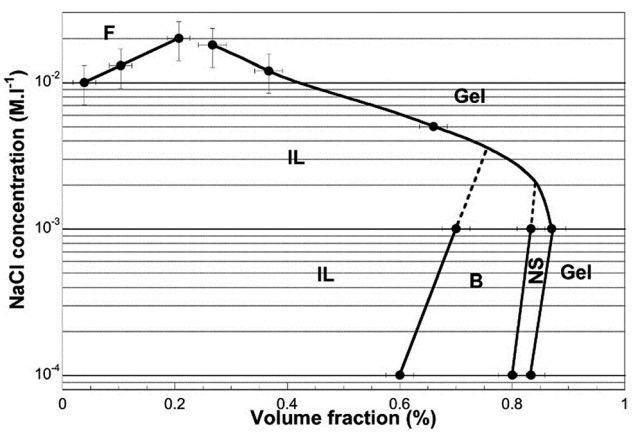

Fig. 8 Phase diagram of sodium nontronite suspensions. Upon increasing volume fraction, the suspensions first form an isotropic liquid (IL), then enter a biphasic regime (B) followed by a small region of nematic sol (NS), and finally form birefringent gels. The line between gel and liquid was determined by oscillatory shear measurements. At high salt concentration, the presence of flocs (F) was checked out by visual observation. Reproduced with permission from Michot *et al.*[21] Copyright (2006) National Academy of Sciences, U.S.A.

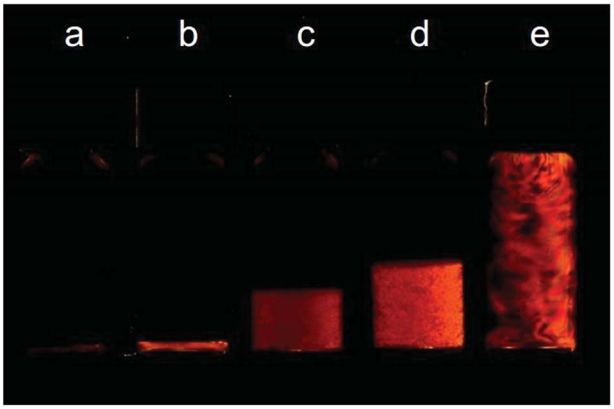

Fig. 9 Aqueous suspensions of nontronite clay NAu-2 observed between cross-polarisers, showing increasing nematic liquid crystal phases volume for clay volume fractions range from 0.5% (a) to 0.72% (d). Sample (e) is a birefringent gel with a volume fraction of 1%. Reproduced with permission from Michot *et al.*[21] Copyright (2006) National Academy of Sciences, U.S.A.

Smectite suspension rheology

As we have noted, smectites form viscous gel phases at low volume fractions, a property which has been widely exploited in a range of industries, from drilling fluids[5] to personal care products.[108] In the sol phase clay suspensions are shear thinning liquids, with increasing shear aligning the anisotropic particles with the flow field. At concentrations above the repulsive gel transition, where the hydrodynamic volumes swept out by the particles overlap, a yield stress develops, and the suspension becomes viscoplastic. The yield stress depends on the clay volume fraction, the particle size,[88] shape,[89,90] and localisation of the charge in the clay layer structure.[109] The gel phase of these particle suspensions is quite "fragile", yielding under small strains of ~1–10 percent, (unlike polymer gels where yield strains of several hundred percent are common). On applying a shear stress above the yielding condition the suspension is transformed into a shear thinning liquid. The complexity of this transformation from solid to liquid-like behaviour can vary significantly with the nature of the smectite clay, as illustrated in Fig. 10.

Ramsay and Lindner[111] showed that static gels of montmorillonite and Laponite had short range spatial and orientational correlations. Under low shear preferential alignment of the larger montmorillonite particles (but not for the smaller Laponite, although elsewhere Pignon[112] did find particle alignments for Laponite at low shear) with the direction of flow, together with the persistence of spatial correlations, suggested structured cooperative flow. Under high shear the spatial correlations were lost, but the orientational alignment was increasingly pronounced. On cessation of flow the spatial correlations reappeared quickly, but the orientational alignment persisted and there was very slow relaxation back to the

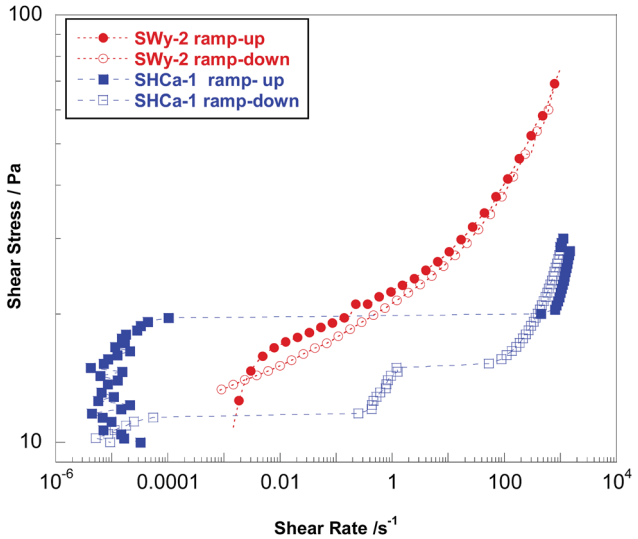

Fig. 10 Controlled-stress shear-rate flow curves for 2.8 wt% hectorite SHCa-1 and 3.2 wt% montmorillonite SWy-2 suspensions at $c > c^*$. Redrawn from data of Ten Brinke *et al.* and Bailey *et al.*[89,110]

isotropic state. This structural relaxation in the suspension was suggested to be the origin of thixotropic behaviour, which is pronounced in smectite gels.[113–115] Thixotropy, often shown as hysteresis loops in flow curves as illustrated in Fig. 11, highlights the importance of shear history and reproducible measurement protocols when studying the rheology of smectite suspensions.[90,116]

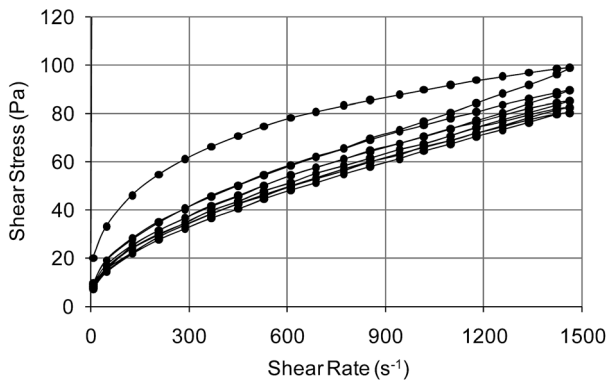

Fig. 11 Shear-stress shear-rate flow curves for montmorillonite suspensions illustrating the dependence of thixotropy on shear history. A preconditioned sample was transferred into the measurement geometry and left at rest for 10 minutes. The shear rate was ramped up then down over the range 11.6–1460 s^{-1} repeatedly for a total of 5 cycles. The total ramp time was 48 min in each direction. The first cycle, the upper loop, shows a breakdown of structure in the gelled suspension which is not fully recovered during the ramp-down. Successive up-down flow curves continue to reduce the level of structure in the suspension and shrink the area of the hysteresis loop until the up and down curves are essentially identical, and two successive loops superimpose on the equilibrium flow curve. Under such conditions, the sample has sufficient time to relax to a steady-state condition at each shear rate and all trace of previous stress history has been removed. Reproduced with permission from Tehrani and Popplestone.[115]

In the attractive gel phase, the enhanced rheology arises from a flocculated network of particles in the suspension.[15] The shear dependent response is characterised by the breakdown of the network into small flocs and individual particles. The association of the particles in different configurations changes the effect on the rheology – at low pH (and moderate ionic strength) edge-face, edge–edge interactions are promoted. As the pH increases and the edge sites deprotonate, the viscosity falls. At higher pH and high electrolyte concentrations face–face van der Waals attraction is enhanced. At low clay concentrations this leads to small flocs and sol destabilisation[23] but at higher concentrations the structure is of overlapping ribbons contributing to higher viscosities[80,117].

Most of the quantification of the rheology of smectite clay suspensions relies on the use of empirical[118,119] or at best semi-empirical[120] models. The links to the underlying physical chemistry and the associated microstructure of the suspensions/gels is often clear qualitatively but it has proved a challenge to obtain quantitative predictive theoretical physicochemical models for understanding and predicting the observed rheology in a similar fashion that has been achieved for polymer systems.[121–126] However, recently some progress in this direction has been made with so-called effective geometrical models,[102,109,127–130] which quantify some of the ideas expressed in this review on the role of the hydrodynamic volume in determining the rheological behaviour of clay systems. These, and related particle simulations,[131–134] should form the basis of more rigorous theoretical understanding and modelling of the rheology of clay-based suspensions and gels in the near future.

Smectite clay-inorganic nanoparticle mixed suspensions

When mixed with other colloidal particles, suspensions of smectite clays exhibit a rich range of behaviour. There is a significant literature in the area of clay nanocomposites where small additives have been used in combination with smectite clays to produce materials with tailored catalytic,[135,136] photochemical,[101,135,137–139] electrical,[140–142] and magnetic[143,144] properties. Here we will focus on the effects of added nanoparticles on phase behaviour and rheological properties. A characteristic of such mixed systems is that the addition of a relatively small amount of the second component can produce significant changes in the behaviour of the suspension. The charge, shape and relative size of the nanoparticles are also important factors in determining the magnitude of the effects observed.

I Smectite clays + spherical nanoparticles

We first consider the situation where the clay and nanoparticle have opposite charges *i.e.* negatively charged clay particles are mixed with positively charged nanoparticles.

I.1 Smectite clay + iron oxide particles. Tombácz and coworkers[145,146] have studied two similar systems: suspensions of 3 wt% montmorillonite containing 0.2 wt% magnetite or 0.15 wt% hematite, both of which are positively charged at the low

pH studied (pH 4). Major enhancements of the shear-thinning rheology were observed, for low relative concentrations of the added nanoparticles (7% and 5% respectively) – see Fig. 12 – due to the enhancement of the clay gel structure by the formation of a heterocoagulated particle network of oppositely charged clay and iron oxide particles. This work also investigated how organic macroions, such as those derived from humic acid, can adsorb on the surface of oxides and reduce or reverse their positive charge, thereby disrupting the hetero-gel structure.

I.2 Smectite clays + cationic silica. Ten Brinke *et al.*[110] carried out a comprehensive study of the rheology, at low ionic strength, of lath-like hectorite (length = 288 nm, width = 43 nm, thickness = 6 nm) dispersions modified by the addition of positively charged alumina-coated silica spheres (Ludox CL, diameter = 17 nm). The suspensions had a total particle concentration of 2.8 wt%, of which 10% (*i.e.* 0.25 wt% in the suspension) was nanoparticles and the remainder hectorite. Addition of the nanoparticle component at this relatively low concentration led to major changes in the rheology of the binary mixtures compared with the pure clay. The mixed suspensions displayed a complex 'yield space' transition from a viscoelastic gel at low applied stresses to a viscous, weakly elastic, shear-thinning liquid at high stresses, see Fig. 13a. The oppositely charged nanoparticles created large mixed particle flocs or percolating networks, depending on the flow/stress regime, by bridging between the clay laths and transforming the repulsive gel of the pure clay to a stronger attractive gel (low stresses) or more viscous liquid (high stresses). Shear moduli, low stress viscosities and effective yield stresses all increased with the addition of silica, with enhancements being up to a factor of 500 and typically 20, depending on the precise rheological characteristic (see Fig. 13a). The large effect of the silica particles reflects the fact that a large number of small spheres can pack effectively around the much larger hectorite laths to form many interparticle bridges.[110]

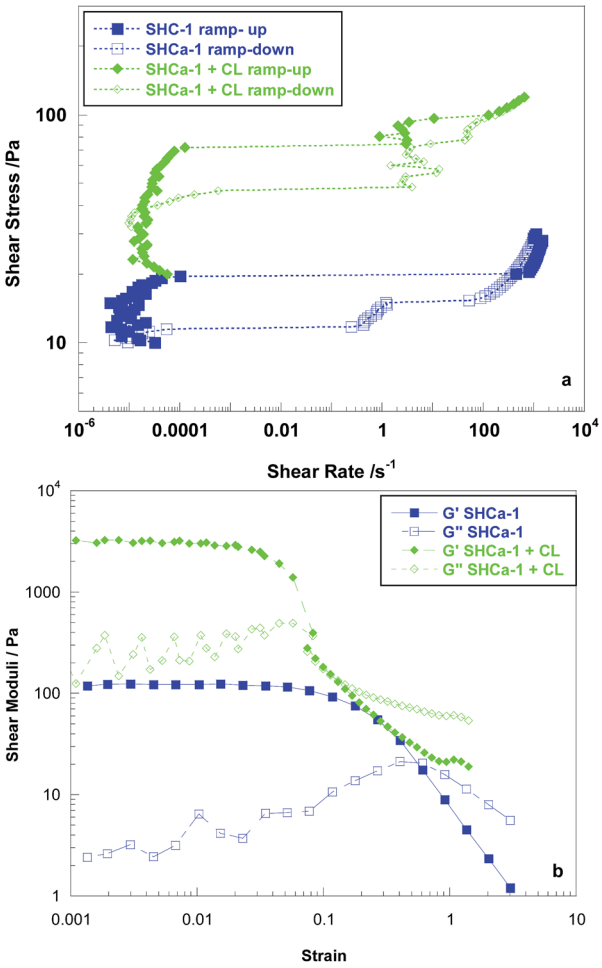

Fig. 13 (a) Controlled-stress continuous shear rheology for 2.8 wt% hectorite suspensions (□) and 2.8 wt% hectorite + 0.25 wt% Ludox CL (◇). Filled symbols: shear stress increasing; open symbols: shear stress decreasing. (b) strain dependence at 1 Hz for storage and loss moduli for 2.8 wt% hectorite suspensions (□) and 2.8 wt% hectorite + 0.25 wt% Ludox CL (◇). Redrawn from Ten Brinke *et al.*[110] with permission.

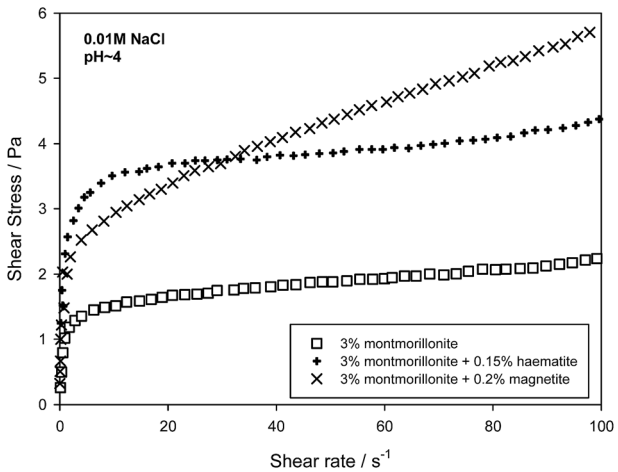

Fig. 12 Flow curves for aqueous montmorillonite clay and iron oxide suspensions with different compositions at pH 4 and low salt concentration. (% = w/w% concentration) Redrawn from Tombácz *et al.*[146]

Bailey *et al.*[89] carried out a similar study where the hectorite clay was replaced by montmorillonite. Here, similar enhancements were observed, albeit somewhat smaller than in the case of hectorite. For example for a suspension at 2.4 wt% total solids, which is just below the overlap concentration of the hydrodynamic volumes of the montmorillonite platelets, addition of 10% Ludox CL increased the low strain elastic modulus from 8 to 30 Pa. Significant increases were also seen in the effective yield stress and viscosity observed in continuous shear flow. At a higher concentration (3.2 wt% total solids), well into the hydrodynamic volume overlap region, replacement of 10% w/w of the clay by Ludox CL increases the shear moduli by a factor of 3. In continuous shear the flow curves show greater shear history dependence, changing from slight thixotropy for the pure clay to marked rheopexy for the mixture.

I.3 Smectite clays + anionic silica. We now consider the situation where the clay and nanoparticle have the same charge sign, *i.e.* where negatively charged clay particles are mixed with negatively charged nanoparticles.

In a series of papers, Lekkerkerker and co-workers[89,110,147,148] looked at the effect of anionic silica nanoparticles on hectorite, montmorillonite and beidellite. At low clay concentrations the silica addition led in general to weaker gels compared to the pure clay system and to incipient phase separation, although the specific manifestation of this differed according to the clay. For hectorite, adding Ludox AS (diameter = 12 nm) Ludox AM (diameter = 15 nm) and Ludox TMA (diameter = 24 nm) to weak low clay concentration gels (0.5 wt% hectorite) leads to the appearance of cracks in the gels followed by a separation into a turbid bottom phase and a clear upper layer. When ~10% w/w Ludox AS40 (diameter = 22 nm) and Ludox TMA was added to montmorillonite SWy-2 at a concentration below the critical hydrodynamic overlap concentration, c^*, of the clay, it was found that the silica nanoparticles destroyed any nascent structure in the fluids, resulting again in phase separation into a turbid lower precipitate and an almost clear upper layer. The effective viscosity was greatly reduced and the rheological hysteresis characteristic of structured fluids virtually eliminated. Addition of Ludox AS 40 to beidellite suspensions forming a nematic liquid crystalline phase caused the concentrations of the coexisting isotropic and nematic phases to be shifted to slightly higher values while at the same time markedly accelerating the phase separation process. Furthermore beidellite suspensions at volume fractions just above the isotropic–nematic phase separation, trapped in a kinetically arrested gel state, liquified on addition of the silica nanospheres and isotropic–nematic phase separation was observed (see Fig. 14).

At higher concentrations where $c > c^*$, the situation is more complicated; in some cases the clay gel is strengthened whereas in others the reverse happens. For hectorite the addition of 0.25 wt% Ludox AS40 to 2.8 wt% hectorite suspensions led to a significant increase of the gel strength. On the other hand, adding Ludox AM and Ludox TMA to strong hectorite gels (2.5 wt% and higher) caused their yield stress and storage modulus to decrease. It therefore appears that the effect of adding like-charged nanoparticles to smectite clays depends strongly on the concentration of the base clay in conjunction with the detailed nature of the silica nanoparticles, for instance their size, surface charge density and accompanying counterions.

Abrahamsson *et al.*[149] studied self-assembled gels in mixed suspensions of nontronite clay plates and silica nanoparticles at different particle concentrations. A strong magnetic field (11.6 Tesla) was used to align the nontronite particles leading to a system with a long-range uniaxial anisotropy.

I.4 Smectite clays + magnetic nanoparticles. Cousin *et al.*[144,150] investigated aqueous mixtures of Laponite RD and silica-coated maghemite nanoparticles. The addition of the silica-coated maghemite spheres shifted the gel transition to much lower Laponite concentrations. Optical microscopy (see Fig. 15) and SANS suggested that the suspension was microphase separated into densely connected domains of gelled Laponite interspersed by liquid-like regions of maghemite. At concentrations just above the gel transition, application of a magnetic field liquefied the system, as deformation of the maghemite domains induced a local mechanical stress to disrupt the gelled Laponite domains.

Mixtures of negatively-charged 12 nm cobalt ferrite nanoparticles with Laponite were considered in a SAXS study by Paula *et al.*[151] In the absence of clay the dilute ferrite particles were stable and non-interacting on a local level. In the presence of Laponite at 0.1 wt%, a slight increase in the structure factor at low Q, similar to that observed by Cousin *et al.* in the Laponite–maghemite system, and visual observations of colour heterogeneity were consistent with a progressive micro phase separation. This was attributed to long range attractive interactions between the ferrite particles induced by the presence of the Laponite particles.

II Smectite clays + rod-like nanoparticles

II.1 Smectite clays + boehmite. Ten Brinke *et al.*[110] also studied mixtures of hectorite with positively charged boehmite rods (length = 200 nm, diameter = 10 nm). As with the alumina coated silica spheres (Ludox CL) the total particle

Fig. 14 Mixed beidellite/silica suspensions observed between crossed polarisers one month after preparation. Volume fraction clay = 0.41%, silica = 0, 0.034, 0.138% from left to right. Reproduced with permission from Landman *et al.*[148] Copyright 2014 American Chemical Society.

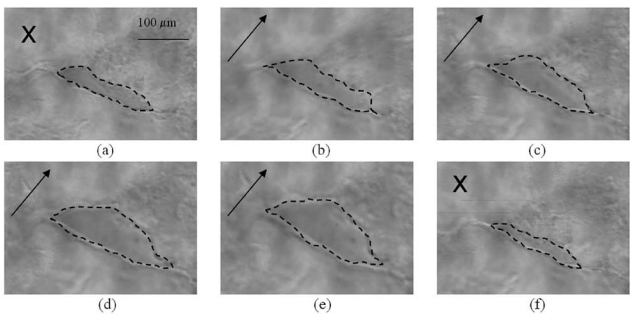

Fig. 15 Observations by optical microscopy of a mixture of Laponite and maghemite (Φmag 0.8%, Φlap 0.38%). (a) A sample at rest 2500 h after synthesis of the mixture. (b–e) Sample under the application of a magnetic field gradient; the pictures are taken at intervals of 1.5 s. (f) Sample at rest after the application of a magnetic field gradient. Reproduced with permission from Cousin *et al.*[144] Copyright 2008 American Chemical Society.

concentration was 2.5 wt% of which 10% was boehmite. The rheological behaviour was qualitatively the same as for hectorite + Ludox CL but the enhancements in elastic modulus, stress dependent viscosity and effective yield stress were significantly lower than for the spherical additive. This reflected the fact that at constant added mass there were significantly fewer boehmite particles per hectorite particle to form interparticle bridges.

Van Der Kooij *et al.*[152] looked at the effect of added boehmite particles on montmorillonite at pH > 10 and in the presence of monovalent salts, where the electrostatic repulsions between particles are suppressed and face–face aggregation is promoted through van der Waals interactions. A significant increase in the yield stress with salinity was observed, going through a maximum at ~15 g L^{-1} NaCl.

II.2 Smectite clays + sepiolite, palygorskite. Mixed clay suspensions such as montmorillonite–palygorskite and montmorillonite–sepiolite have attracted interest[153–155] as these minerals are often co-deposited. Here, where the particles are of comparable size, shape plays a key role in the effect on rheology, with addition of the second component initially at low concentrations fitting into the random repulsive gel network, as exemplified by a small increase in rheology for low concentrations, then at larger concentrations disrupting the packing leading to a deterioration in rheological parameters. This behaviour is illustrated in Fig. 16. The effect on rheology has been strongly correlated with layer charge,[155] where higher layer charge favours assembly of the clay sheets into multilamellar aggregates, reducing the effective surface available for bridging interactions between clay particles.

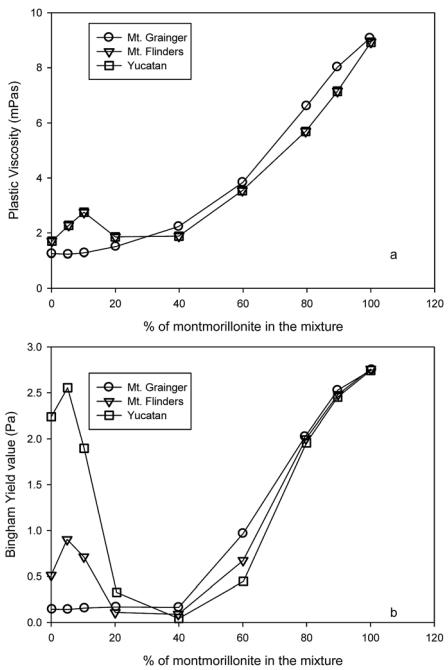

Fig. 16 Effect of montmorillonite concentration on plastic viscosity (a) and Bingham yield value (b) of mixed suspensions of Na-saturated palygorskite and montmorillonite at a total clay concentration of 3% w/v and pH 7. Redrawn with permission from Neaman & Singer.[153]

III Smectite clays + plate-like nanoparticles

III.1 Smectite clays + mixed metal hydroxides. Mixed-metal hydroxides (MMH), often referred to as layered double hydroxides, are the cationic analogues to the smectite clays, consisting of layers of positively charged hydroxide octahedra, with interlayer anions. Hydrotalcite, magnesium aluminium hydroxide, is the most common MMH, with the general formula $[Mg_{1-x}Al_x(OH)_2]^{x+}A_{x/n}{}^{n-}\cdot mH_2O$. Natural and synthetic hydrotalcites are found with x varying between 0.2 and 0.4 (ref. 156). Synthetic hydrotalcites are generally produced by a co-precipitation method giving small hexagonal crystals of face diameter ~10–100 nm (ref. 157).

Burba *et al.*[158–160] considered for drilling fluid applications the addition of hydrotalcite to montmorillonite clay at a mass ratio of 1 : 10, where an enhancement in the rheology was observed. The mixture of positively charged hydrotalcite with the negatively charged clay resulted in a heteroflocculated system, with the enhanced rheology arising from the flocculated particle network.[161,162] Build-up of the network structure was followed through the evolution of viscosity or elasticity in the suspension as a function of time after a period of high shear, and it was observed that the time scales for this were much more rapid with the presence of the small hydrotalcite particles. This is probably due to the more rapid Brownian rotational and translation diffusion of the smaller particles being reflected in the more rapid thixotropic response.[111]

Lagaly and co-workers[156,163] showed sharp maxima in the yield stress and viscosity of mixed montmorillonite–hydrotalcite suspensions as a function of hydrotalcite particle mass fraction, with the peak in the rheology coinciding with 1 : 1 equivalence of cationic and anionic surface charge (see Fig. 17).

Subsequently Hou and co-workers[164–167] have carried out extensive investigations of the thixotropic behaviour of mixed montmorillonite–hydrotalcite suspensions. They observe three general types of behaviour which they term (a) positive thixotropy, time-dependent shear thinning; (b) negative thixotropy, time-dependent shear thickening; and (c) complex thixotropy, where the system displays a combination of negative and positive thixotropy with increasing time. They have shown that the precise thixotropy behaviour is a complex function of the

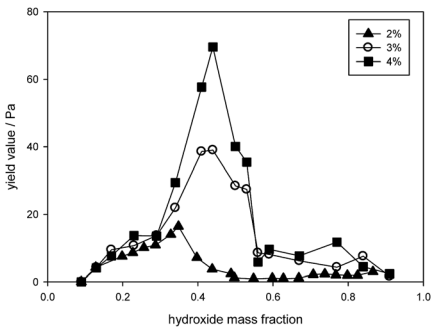

Fig. 17 Yield value of heterocoagulated dispersions of montmorillonite and magnesium aluminium oxide with 2 (▲), 3 (○), and 4 (■) wt% solids contents as a function of the hydroxide mass fraction. Redrawn with permission from Lagaly *et al.*[163]

total clay/hydrotalcite particle concentration, the hydrotalcite–montmorillonite ratio, electrolyte concentration and type and suggest possible mechanisms due to changes in particle interactions and microstructure.

A further study of the effect of clay particle size on mixed hydrotalcite–montmorillonite systems in the context of drilling fluid applications has been carried out by Baruah *et al.*[168]

So far we have discussed the effect of adding mixed metal hydroxides on montmorillonite suspensions. However, similar enhanced rheological effects have been observed for other smectite clay systems, including hectorite[169] and Laponite.[170] This highlights the generic effect of MMH in enhancement of smectite clay rheology.

III.2 Smectite clays + gibbsite. Ten Brinke *et al.*[110] investigated the rheological enhancement of hectorite gels by gibbsite plates in comparison to Ludox CL spheres and boehmite rods discussed earlier. The rheological enhancement observed with gibbsite was inferior to that observed with cationic silica, but superior to that observed with boehmite. This has been rationalised by Ten Brinke *et al.* on the basis of the competition between the better packing of the gibbsite plate particles around the hectorite laths compared with the boehmite rods, and greater number density of the Ludox CL. The effectiveness of the different shape particles' face–face bridging between the hectorite particles is also reflected in the strain sensitivity of the particle network, with the yield strain decreasing with the maximum dimension of the bridging particle.

In addition to their work on boehmite, Van Der Kooij *et al.*[152] looked at the effect of added gibbsite on montmorillonite at pH > 10 and in the presence of monovalent salts, where again the electrostatic repulsions between particles are suppressed and face–face aggregation is promoted through van der Waals interactions. In this case a significant increase in the yield stress was observed, with maximum yield stresses attained at ~18 g L^{-1} NaCl. On a weight for weight basis gibbsite was found to be significantly more effective as an additive than boehmite, in line with the similar findings for the hectorite system.

These workers compared this performance to that obtained with salt-free MMH heteroflocculated montmorillonite suspensions of the type studied by Burba[159] and Lange.[171] Fig. 18 shows that the degree of rheology enhancement from the van der Waals flocculated systems is comparable to that of the heteroflocculated system and has the benefit of increased robustness in the presence of high salinity.

III.3 Smectite clays + Laponite. Mixtures of Laponite-montmorillonite[172] form cooperative gels with significantly enhanced rheological properties. In near equal mass ratios the two components appear to form a homogenously structured network with a close interaction between Laponite and montmorillonite, but with either component in excess (1 : 2, 2 : 1 by weight) considerable heterogeneity and structural anisotropy are observed. The same authors[173] investigated the dynamics of the gelation/aging process and found a rapid early stage dominated by the smaller Laponite dynamics followed by a slower process reflecting the slower montmorillonite dynamics.

III.4 Smectite clays + clay hybrids. Jung *et al.*[136] studied the effect of pillared clay additives on the rheology of

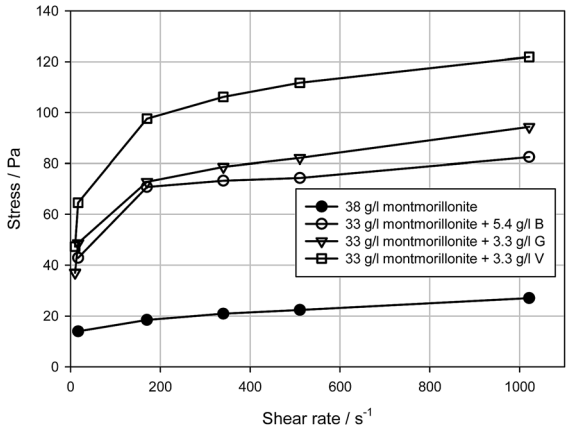

Fig. 18 Shear stress/shear rate flow curves for suspensions of montmorillonite (bentonite) and montmorillonite–MMH(V) in fresh water, compared with montmorillonite–gibbsite (G) and montmorillonite–boehmite (B) in 15 g L^{-1} NaCl. Redrawn from van der Kooij *et al.*[152]

montmorillonite suspensions. They used two additives, both pillared montmorillonite aggregates, one interacted with iron oxide and the other with an aluminosilica. The charge on the former was slightly negative at low pH rising to positive values above pH 8, whilst the latter was more negatively charged than the base montmorillonite even at pH 5 and acquired an increasingly negative zeta potential with increasing pH. As a result of this, when 0.5 wt% of additive was added to a 5 wt% montmorillonite suspension, the rheological properties (storage modulus, shear-dependent viscosity, yield stress and yield strain) all increased dramatically for the iron oxide modified particle (G′ for example increased by an order of magnitude, as shown in Fig. 19, and the yield stress from 1.3 Pa to 12 Pa), whereas above pH 6 the corresponding values for the aluminosilica aggregate additive were dramatically reduced compared to the base clay suspension – the gel was effectively destroyed. Cryo-TEM images of the suspension structure were consistent with the iron oxide case having a heteroflocculated

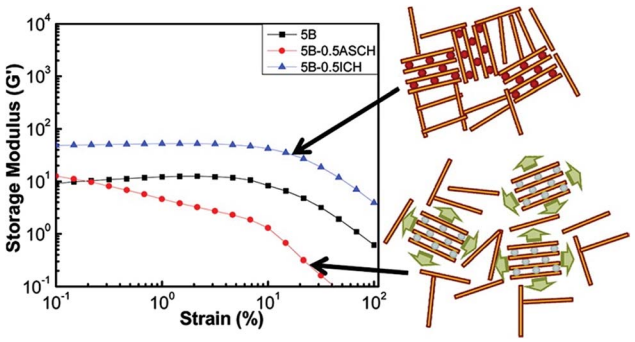

Fig. 19 Storage modulus as function of strain for aqueous suspensions of 5 wt% montmorillonite (5B), 5 wt% montmorillonite + 0.5 wt% alumina-silica clay hybrid (5B-0.5ASCH) and 5 wt% montmorillonite + 0.5 wt% iron oxide nanoparticle clay hybrid (5B-0.5ICH). Reproduced by permission from Jung el al.[136] Copyright 2011 American Society of Chemistry.

reinforced gel structure, whereas the aluminosilicate case had a much looser, locally flocculated structure than the base clay. Possible microstructures consistent with these images and the observed bulk property modifications are illustrated in Fig. 19. High temperature high pressure rheology measurements showed that the high temperature enhanced gelation effects commonly observed for montmorillonite suspensions (due to increases in ionic strength by sodium silicate dissolution) were reinforced by the iron oxide additive and essentially removed by the aluminosilicate additive.

III.5 Smectite clays + layered niobates and titanates. Nakato and Miyamoto and co-workers considered mixtures of niobate[137,138] and titanate[174,175] nanosheets with smectite clays (montmorillonite and Laponite). In all cases the liquid crystalline behaviour of the pure nanosheets persists in the mixtures, and is even enriched by an additional nematic phase for titanate–Laponite, despite the fact that the clay and nano sheets segregate at the microscopic scale. This segregation behaviour leads to a stabilised photoelectric charge separated state which can be exploited in photocatalysis applications. The richness of phase behaviour observed for the titanate–Laponite system is shown in Fig. 20.

Overarching themes and conclusions

1. For binary mixtures with components of opposite charge, the extent of the rheology enhancements created by the added nanoparticles through the formation of a hetero-flocculated extended clay attractive gel network is determined by (a) the number of added particles, which determines the number of potential bridges or crosslinks and (b) the ability of the added nanoparticles to pack efficiently around the clay particles as determined by their effective hydrodynamic volumes, which is largely determined by their largest dimension. In general spherical particles can pack more efficiently around smectite clay platelets or laths, and smaller plates will pack more effectively than longer rods.

2. For these gels with components of opposite charge, the yield strain appears to correlate with the maximum dimension of the small bridging particles. This is consistent with the particle bridging mechanism.

3. For gels reinforced by the clay-nanoparticle electrostatic attractive interactions, the effects diminish rapidly as salt is added and the ionic strength increases, screening out the electrostatic interactions. However, under these conditions gel enhancement can still be achieved by using nanoparticles such as gibbsite and boehmite for which the clay-nanoparticle van der Waals attractive forces are significant and give rise to attractive bridging even at high salinities.

4. For like charged clay-nanoparticle binary mixtures, gel reinforcement and rheological enhancement can still take place but occurs by a different mechanism. Here, the small nanoparticles may act as depletants[176] and cause attractive forces between the clay particles to enhance the clay network.

5. For some clay-nanoparticle systems, the attractive depletion interactions arising from the presence of the smaller component drive phase separation and result in a fractionation of the particles according to their shape. The fractionated components form liquid crystalline domains that are structurally distinct from one another and reflect the shape of the dominant particle.

6. However, this behaviour is far from universal and is not even the norm. It is observed that when anionic silica particles are added to the smectite clays, they influence the gel formation but with different outcomes. For montmorillonite and hectorite, the gels can become stronger or weaker through the interactions caused by the additive, depending on the clay concentration and the precise nature of the silica. For beidellite anionic silica breaks up the gel and drives phase separation into a nematic phase.

7. In niobate and titanate large plate (~1–10 μm) systems where the added component is a clay (montmorillonite or Laponite respectively), it is the clay that acts as the depletant for the sheet-like particles. Here these interactions modulate the phase behaviour of the pure niobate/titanate suspensions to give an even richer tapestry of liquid crystalline phases than for the pure components.

8. For binary mixtures where the second component is also a clay of comparable size, a key factor determining whether the gel is enhanced or disrupted is the ability of one clay to fit efficiently into the gel structure of the other clay. Here there is a balance between reinforcement of the repulsive gel by adding a second component of similar charge and the degree of geometrical disruption of the gel due to the contrast of shape and size.

9. Likewise, for montmorillonite and the larger sepiolite rods (or needles), the montmorillonite modifies the rheological behaviour of the sepiolite suspension. A small addition of montmorillonites reinforces the mixed gel structure and enhances the viscosity and other rheological characteristics.

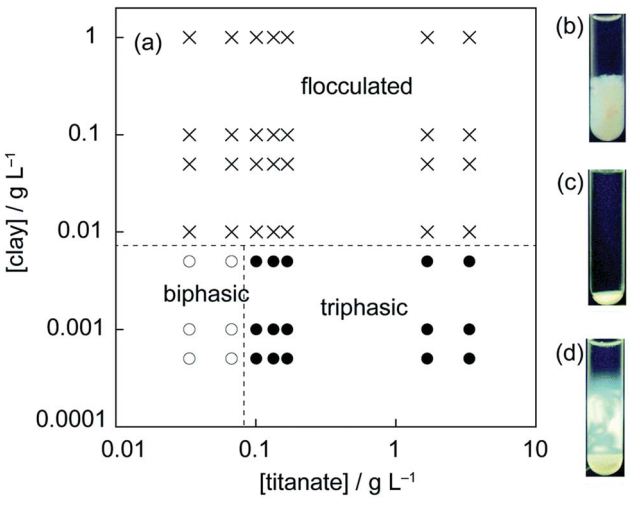

Fig. 20 (a) Phase diagram of the titanate–clay binary nanosheet colloids, and typical appearances of the (b) flocculated, (c) isotropic–LC biphasic, and (d) isotropic–LC–LC triphasic samples between crossed polarizers. Symbols embedded in the diagram indicate experimentally examined compositions. Reproduced from Nakato *et al.*[175]

However, beyond ~10% addition of plates, the packing disruption of the sepiolite rod gel structure results in a reduction of viscosity towards the lower limiting value of the pure montmorillonite system.

10. There are major pH effects in the behaviour of the binary mixtures; the charge and its pH dependence of the added particles compared with the charge and pH dependence of the edge charges of the clay can determine whether there is gel reinforcement through bridging by a net positive–negative interaction between the components or gel weakening and liquefaction due to net negative–negative interactions where the size difference and overall particle concentration drives the system to local aggregate formation rather than formation of a repulsive gel.

We hope that this review makes it clear that smectite clay-inorganic nanoparticle suspensions offer fantastic opportunities to produce materials with new and fascinating properties and at the same time present significant scientific challenges. Further progress in this field requires work on well-characterised systems using a combination of experimental techniques to measure structure (both in real and reciprocal space) and dynamics, in combination with analysis in terms of relevant theory. Once we understand the rules from model systems, we can better exploit these systems for commercial applications by tailoring properties using cheap and abundantly available materials.

Acknowledgements

We thank all our collaborators and colleagues, who are essential for our continued efforts and interest in this field, for their interest, input and valuable discussions.

Notes and references

1 I. E. Odom, *Philos. Trans. R. Soc. London*, 1984, 391–409.
2 H. H. Murray, *Appl. Clay Sci.*, 2000, **17**, 207–221.
3 F. Bergaya, B. K. G. Theng and G. Lagaly, *Handbook of clay science*, Elsevier B.V., 2006.
4 G. Lagaly, *Bentonites: Adsorbents of toxic substances*, Springer-Verlag GmbH & Company KG, Julich, Ger, 1994.
5 R. Caenn, H. C. H. Darley and G. R. Gray, *Composition and properties of drilling and completion fluids*, Gulf Publishing Company, Saint Louis, MO, USA, 6th edn, 2011.
6 T. J. Pinnavaia and G. W. Beall, *Polymer-clay nanocomposites*, Wiley, 2001.
7 G. W. Brindley and G. Brown, *Crystal structures of clay minerals and their x-ray identification*, Mineralogical Society, 1980.
8 N. Güven, *Rev. Mineral. Geochem.*, 1988, **19**, 497–559.
9 B. Velde, *Introduction to clay minerals*, 1992.
10 J. T. Kloprogge, S. Komarneni and J. E. Amonette, *Clays Clay Miner.*, 1999, **47**, 529–554.
11 A. Meunier and N. Fradin, *Clays*, Springer, 2005.
12 N. Güven, *Elements*, 2009, **5**, 89–92.
13 F. Wolters, G. Lagaly, G. Kahr, R. Nueesch and K. Emmerich, *Clays Clay Miner.*, 2009, **57**, 115–133.
14 H. Van Olphen, *An introduction to clay colloid chemistry: For clay technologists, geologists, and soil scientists*, Wiley, 1977.
15 P. F. Luckham and S. Rossi, *Adv. Colloid Interface Sci.*, 1999, **82**, 43–92.
16 G. Sposito, N. T. Skipper, R. Sutton, S. H. Park, A. K. Soper and J. A. Greathouse, *Proc. Natl. Acad. Sci. U. S. A.*, 1999, **96**, 3358–3364.
17 N. Güven and R. M. Pollastro, *Clay–water interface and its rheological implications*, The Clay Minerals Society, 1992.
18 J. C. P. Gabriel, C. Sanchez and P. Davidson, *J. Phys. Chem.*, 1996, **100**, 11139–11143.
19 S. Abend and G. Lagaly, *Appl. Clay Sci.*, 2000, **16**, 201–227.
20 P. Davidson and J. C. P. Gabriel, *Curr. Opin. Colloid Interface Sci.*, 2005, **9**, 377–383.
21 L. J. Michot, I. Bihannic, S. Maddi, S. S. Funari, C. Baravian, P. Levitz and P. Davidson, *Proc. Natl. Acad. Sci. U. S. A.*, 2006, **103**, 16101–16104.
22 B. Ruzicka and E. Zaccarelli, *Soft Matter*, 2011, **7**, 1268–1286.
23 G. Lagaly and S. Ziesmer, *Adv. Colloid Interface Sci.*, 2003, **100–102**, 105–128.
24 L. J. Michot, I. Bihannic, F. Thomas, B. S. Lartiges, Y. Waldvogel, C. Caillet, J. Thieme, S. S. Funari and P. Levitz, *Langmuir*, 2013, **29**, 3500–3510.
25 G. Brown, *Philos. Trans. R. Soc. London*, 1984, 221–240.
26 J. M. Saunders, J. W. Goodwin, R. M. Richardson and B. Vincent, *J. Phys. Chem. B*, 1999, **103**, 9211–9218.
27 E. Paineau, A. M. Philippe, K. Antonova, I. Bihannic, P. Davidson, I. Dozov, J. C. P. Gabriel, M. Impéror-Clerc, P. Levitz, F. Meneau and L. J. Michot, *Liquid Crystals Reviews*, 2013, **1**, 110–126.
28 R. E. Grim, *Clay mineralogy*, McGraw-Hill, 1953.
29 R. B. Secor and C. J. Radke, *J. Colloid Interface Sci.*, 1985, **103**, 237–244.
30 E. Tombácz and M. Szekeres, *Appl. Clay Sci.*, 2004, **27**, 75–94.
31 F. R. C. Chang and G. Sposito, *J. Colloid Interface Sci.*, 1996, **178**, 555–564.
32 M. Duc, F. Gaboriaud and F. Thomas, *J. Colloid Interface Sci.*, 2005, **289**, 139–147.
33 M. Duc, F. Gaboriaud and F. Thomas, *J. Colloid Interface Sci.*, 2005, **289**, 148–156.
34 M. Delhorme, C. Labbez, C. Caillet and F. Thomas, *Langmuir*, 2010, **26**, 9240–9249.
35 L. M. Barclay and R. H. Ottewill, *Spec. Discuss. Faraday Soc.*, 1970, **1**, 138–147.
36 S. D. Lubetkin, S. R. Middleton and R. H. Ottewill, *Philos. Trans. R. Soc. London*, 1984, 353–368.
37 P. Fletcher and G. Sposito, *Clay Miner.*, 1989, **24**, 375–391.
38 P. L. Hall and D. M. Astill, *Clays Clay Miner.*, 1989, **37**, 355–363.
39 J. H. Denis, *Clays Clay Miner.*, 1991, **39**, 35–42.
40 J. H. Denis, M. J. Keall, P. L. Hall and G. H. Meeten, *Clay Miner.*, 1991, **26**, 255–268.
41 A. Delville, *Langmuir*, 1991, **7**, 547–555.
42 A. Delville, *Langmuir*, 1992, **8**, 1796–1805.

43 J. M. Cases, I. Bérend, G. Besson, M. François, J. P. Uriot, F. Thomas and J. E. Poirier, *Langmuir*, 1992, **8**, 2730–2739.
44 E. S. Boek, P. V. Coveney and N. T. Skipper, *J. Am. Chem. Soc.*, 1995, **117**, 12608–12617.
45 E. S. Boek, P. V. Coveney and N. T. Skipper, *Langmuir*, 1995, **11**, 4629–4631.
46 N. T. Skipper, C. Fang-Ru Chou and G. Sposito, *Clays Clay Miner.*, 1995, **43**, 285–293.
47 N. T. Skipper, G. Sposito and C. Fang-Ru Chou, *Clays Clay Miner.*, 1995, **43**, 294–303.
48 S. Karaborni, B. Smit, W. Heidug, J. Urai and E. Van Oort, *Science*, 1996, **271**, 1102–1104.
49 J. M. Cases, I. Bérend, M. François, J. P. Uriot, L. J. Michot and F. Thomas, *Clays Clay Miner.*, 1997, **45**, 8–22.
50 D. A. Laird, *Clays Clay Miner.*, 1999, **47**, 630–636.
51 E. J. M. Hensen and B. Smit, *J. Phys. Chem. B*, 2002, **106**, 12664–12667.
52 E. S. Boek and M. Sprik, *J. Phys. Chem. B*, 2003, **107**, 3251–3256.
53 V. Marry and P. Turq, *J. Phys. Chem. B*, 2003, **107**, 1832–1839.
54 T. J. Tambach, E. J. M. Hensen and B. Smit, *J. Phys. Chem. B*, 2004, **108**, 7586–7596.
55 N. Malikova, A. Cadène, V. Marry, E. Dubois and P. Turq, *J. Phys. Chem. B*, 2006, **110**, 3206–3214.
56 E. Ferrage, B. Lanson, B. A. Sakharov, N. Geoffroy, E. Jacquot and V. A. Drits, *Am. Mineral.*, 2007, **92**, 1731–1743.
57 B. Rotenberg, V. Marry, R. Vuilleumier, N. Malikova, C. Simon and P. Turq, *Geochim. Cosmochim. Acta*, 2007, **71**, 5089–5101.
58 R. L. Anderson, I. Ratcliffe, H. C. Greenwell, P. A. Williams, S. Cliffe and P. V. Coveney, *Earth-Sci. Rev.*, 2010, **98**, 201–216.
59 M. Segad, B. Jönsson, T. Åkesson and B. Cabane, *Langmuir*, 2010, **26**, 5782–5790.
60 E. S. Boek, *Mol. Phys.*, 2014, **112**, 1472–1483.
61 K. Norrish, *Discuss. Faraday Soc.*, 1954, **18**, 120–134.
62 J. P. Quirk, in *Advances in agronomy*, ed. L. S. Donald, Academic Press, 1994, vol. 53, pp. 121–183.
63 M. B. McBride and P. Baveye, *Soil Sci. Soc. Am. J.*, 2002, **66**, 1207–1217.
64 J. P. Quirk, M. B. McBride and P. Baveye, *Soil Sci. Soc. Am. J.*, 2003, **67**, 1960–1964.
65 M. V. Smalley, *Mol. Phys.*, 1990, **71**, 1251–1267.
66 I. S. Sogami, T. Shinohara and M. V. Smalley, *Mol. Phys.*, 1991, **74**, 599–612.
67 I. S. Sogami, T. Shinohara and M. V. Smalley, *Mol. Phys.*, 1992, **76**, 1–19.
68 J. T. G. Overbeek, *Mol. Phys.*, 1993, **80**, 685–694.
69 M. V. Smalley and I. S. Sogami, *Mol. Phys.*, 1995, **85**, 869–881.
70 R. J. M. Pellenq, N. Lequeux and H. van Damme, *Cem. Concr. Res.*, 2008, **38**, 159–174.
71 H. Freundlich, *Kolloid-Z.*, 1928, **46**, 289–299.
72 G. Broughton and L. Squires, *J. Phys. Chem.*, 1936, **40**, 1041–1053.
73 E. A. Hauser and C. E. Reed, *J. Phys. Chem.*, 1936, **40**, 1169–1182.
74 H. Freundlich, *J. Phys. Chem.*, 1937, **41**, 901–910.
75 E. A. Hauser and C. E. Reed, *J. Phys. Chem.*, 1937, **41**, 911–934.
76 E. A. Hauser and D. S. Le Beau, *J. Phys. Chem.*, 1938, **42**, 961–969.
77 I. Langmuir, *J. Chem. Phys.*, 1938, **6**, 873–896.
78 H. Van Olphen, *Discuss. Faraday Soc.*, 1951, **11**, 82–84.
79 H. Van Olphen, *Trans. Faraday Soc.*, 1958, **54**, 144.
80 H. Vali and L. Bachmann, *J. Colloid Interface Sci.*, 1988, **126**, 278–291.
81 M. Morvan, D. Espinat, J. Lambard and T. Zemb, *Colloids Surf., A*, 1994, **82**, 193–203.
82 I. Bihannic, L. J. Michot, B. S. Lartiges, D. Vantelon, J. Labille, F. Thomas, J. Susini, M. Salome and B. Fayard, *Langmuir*, 2001, **17**, 4144–4147.
83 A. Shalkevich, A. Stradner, S. K. Bhat, F. Mulle and P. Schurtenberger, *Langmuir*, 2007, **23**, 3570–3580.
84 M. S. Zbik, R. L. Frost and Y. F. Song, *J. Colloid Interface Sci.*, 2008, **319**, 169–174.
85 M. S. Zbik, R. L. Frost, Y. F. Song, Y. M. Chen and J. H. Chen, *J. Colloid Interface Sci.*, 2008, **319**, 457–461.
86 M. S. Zbik, W. N. Martens, R. L. Frost, Y. F. Song, Y. M. Chen and J. H. Chen, *Langmuir*, 2008, **24**, 8954–8958.
87 Y. Cui, C. L. Pizzey and J. S. Van Duijneveldt, *Philos. Trans. R. Soc., A*, 2013, **371**, 20120262.
88 L. J. Michot, I. Bihannic, K. Porsch, S. Maddi, C. Baravian, J. Mougel and P. Levitz, *Langmuir*, 2004, **20**, 10829–10837.
89 L. Bailey, H. N. W. Lekkerkerker and G. C. Maitland, *Rheol. Acta*, 2014, **53**, 373–384.
90 A. J. W. Ten Brinke, L. Bailey, H. N. W. Lekkerkerker and G. C. Maitland, *Soft Matter*, 2007, **3**, 1145–1162.
91 A. Mourchid, A. Delville, J. Lambard, E. Lécolier and P. Levitz, *Langmuir*, 1995, **11**, 1942–1950.
92 A. Mourchid, A. Delville and P. Levitz, *Faraday Discuss.*, 1995, **101**, 275–285.
93 A. Mourchid, E. Lécolier, H. Van Damme and P. Levitz, *Langmuir*, 1998, **14**, 4718–4723.
94 P. Levitz, E. Lécolier, A. Mourchid, A. Delville and S. Lyonnard, *Europhys. Lett.*, 2000, **49**, 672–677.
95 D. Bonn, H. Tanaka, P. Coussot and J. Meunier, *J. Phys.: Condens. Matter*, 2004, **16**, S4987–4992.
96 B. Ruzicka, L. Zulian and G. Ruocco, *Langmuir*, 2006, **22**, 1106–1111.
97 E. Lécolier, PhD Thesis, Université d'Orleans, 1998.
98 D. M. Fonseca, Y. Méheust, J. O. Fossum, K. D. Knudsen, K. J. Måløy and K. P. S. Parmar, *J. Appl. Crystallogr.*, 2007, **40**, s292–s296.
99 H. Hemmen, N. I. Ringdal, E. N. De Azevedo, M. Engelsberg, E. L. Hansen, Y. Méheust, J. O. Fossum and K. D. Knudsen, *Langmuir*, 2009, **25**, 12507–12515.
100 N. I. Ringdal, D. M. Fonseca, E. L. Hansen, H. Hemmen and J. O. Fossum, *Phys. Rev. E: Stat., Nonlinear, Soft Matter Phys.*, 2010, **81**, 014702.
101 N. Miyamoto, H. Iijima, H. Ohkubo and Y. Yamauchi, *Chem. Commun.*, 2010, **46**, 4166–4168.

102 L. J. Michot, E. Paineau, I. Bihannic, S. Maddi, J. F. L. Duval, C. Baravian, P. Davidson and P. Levitz, *Clay Miner.*, 2013, **48**, 663–685.
103 E. Paineau, K. Antonova, C. Baravian, I. Bihannic, P. Davidson, I. Dozov, M. Impéror-Clerc, P. Levitz, A. Madsen, F. Meneau and L. J. Michot, *J. Phys. Chem. B*, 2009, **113**, 15858–15869.
104 L. Onsager, *Annu. Rev. Phys. Chem.*, 1949, **51**, 627–659.
105 J. A. C. Veerman and D. Frenkel, *Phys. Rev. A*, 1992, **45**, 5632–5648.
106 W. F. Bleam, *Clays Clay Miner.*, 1990, **38**, 527–536.
107 M. Delhorme, B. Jonsson and C. Labbez, *RSC Adv.*, 2014, **4**, 34793–34800.
108 D. B. Braun and M. R. Rosen, *Rheology modifiers handbook - practical use and application*, William Andrew Publishing, 2000.
109 E. Paineau, L. J. Michot, I. Bihannic and C. Baravian, *Langmuir*, 2011, **27**, 7806–7819.
110 A. J. W. Ten Brinke, L. Bailey, H. N. W. Lekkerkerker and G. C. Maitland, *Soft Matter*, 2008, **4**, 337–348.
111 J. D. F. Ramsay and P. Lindner, *J. Chem. Soc., Faraday Trans.*, 1993, **89**, 4207–4214.
112 F. Pignon, A. Magnin, J. M. Piau, B. Cabane, P. Lindner and O. Diat, *Phys. Rev. E: Stat. Phys., Plasmas, Fluids, Relat. Interdiscip. Top.*, 1997, **56**, 3281–3289.
113 D. C. H. Cheng and F. Evans, *Br. J. Appl. Phys.*, 1965, **16**, 1599–1617.
114 N. J. Alderman, A. Gavignet, D. Guillot and G. C. Maitland, *SPE 18035, 63rd Annual Technical Conference and Exhibition of the Society of Petroleum Engineers*, Houston, Tx., USA., 1988.
115 A. Tehrani and A. Popplestone, *AADE-2009-NTCE-12-02, AADE 2009 National Technical Conference & Exhibition*, New Orleans, Louisiana, 2009.
116 P. C. F. Moller, J. Mewis and D. Bonn, *Soft Matter*, 2006, **2**, 274–283.
117 A. Weiss and R. Frank, *Kolloid-Z.*, 1961, **177**, 47–56.
118 W. H. Herschel and R. Bulkley, *Kolloid-Z.*, 1926, **39**, 291–300.
119 E. C. Bingham, *J. Chem. Educ.*, 1929, **6**, 1206–1214.
120 I. M. Krieger and T. J. Dougherty, *Trans. Soc. Rheol.*, 1959, **3**, 137–152.
121 M. Doi and S. F. Edwards, *J. Chem. Soc., Faraday Trans. 2*, 1978, **74**, 1789–1801.
122 M. Doi and S. F. Edwards, *J. Chem. Soc., Faraday Trans. 2*, 1978, **74**, 1802–1817.
123 M. Doi and S. F. Edwards, *J. Chem. Soc., Faraday Trans. 2*, 1978, **74**, 1818–1832.
124 M. Doi and S. F. Edwards, *J. Chem. Soc., Faraday Trans. 2*, 1979, **75**, 38–54.
125 M. Doi, J. I. Takimoto, P. G. De Gennes, R. Magerle, A. N. Semenov, D. J. Read, M. E. Cates and X. H. Zheng, *Philos. Trans. R. Soc., A*, 2003, **361**, 641–652.
126 G. Marrucci, G. Ianniruberto, A. E. Likhtman and M. E. Cates, *Philos. Trans. R. Soc., A*, 2003, **361**, 677–688.
127 D. Quemada, *Eur. Phys. J.: Appl. Phys.*, 1998, **1**, 119–127.
128 C. Baravian, D. Vantelon and F. Thomas, *Langmuir*, 2003, **19**, 8109–8114.
129 L. J. Michot, C. Baravian, I. Bihannic, S. Maddi, C. Moyne, J. F. L. Duval, P. Levitz and P. Davidson, *Langmuir*, 2009, **25**, 127–139.
130 A. M. Philippe, C. Baravian, V. Bezuglyy, J. R. Angilella, F. Meneau, I. Bihannic and L. J. Michot, *Langmuir*, 2013, **29**, 5315–5324.
131 E. S. Boek, P. V. Coveney, H. N. W. Lekkerkerker and P. Van Der Schoot, *Phys. Rev. E: Stat. Phys., Plasmas, Fluids, Relat. Interdiscip. Top.*, 1997, **55**, 3124–3133.
132 Q. Meng and J. J. L. Higdon, *J. Rheol.*, 2008, **52**, 37–65.
133 Q. Meng and J. J. L. Higdon, *J. Rheol.*, 2008, **52**, 1–36.
134 E. Dickinson, *Adv. Colloid Interface Sci.*, 2013, **199–200**, 114–127.
135 K. Mogyorósi, I. Dékány and J. H. Fendler, *Langmuir*, 2003, **19**, 2938–2946.
136 Y. Jung, Y. H. Son, J. K. Lee, T. X. Phuoc, Y. Soong and M. K. Chyu, *ACS Appl. Mater. Interfaces*, 2011, **3**, 3515–3522.
137 N. Miyamoto and T. Nakato, *Langmuir*, 2003, **19**, 8057–8064.
138 N. Miyamoto, Y. Yamada, S. Koizumi and T. Nakato, *Angew. Chem., Int. Ed.*, 2007, **46**, 4123–4127.
139 T. Nakato and N. Miyamoto, *Materials*, 2009, **2**, 1734–1761.
140 C. Nethravathi, B. Viswanath, C. Shivakumara, N. Mahadevaiah and M. Rajamathi, *Carbon*, 2008, **46**, 1773–1781.
141 Y. F. Lan and J. J. Lin, *J. Phys. Chem. A*, 2009, **113**, 8654–8659.
142 S. Santangelo, G. Gorrasi, R. Di Lieto, S. De Pasquale, G. Patimo, E. Piperopoulos, M. Lanza, G. Faggio, F. Mauriello, G. Messina and C. Milone, *Appl. Clay Sci.*, 2011, **53**, 188–194.
143 C. Galindo-Gonzalez, J. De Vicente, M. M. Ramos-Tejada, M. T. Lopez-Lopez, F. Gonzalez-Caballero and J. D. G. Duran, *Langmuir*, 2005, **21**, 4410–4419.
144 F. Cousin, V. Cabuil, I. Grillo and P. Levitz, *Langmuir*, 2008, **24**, 11422–11430.
145 E. Tombácz, C. Csanaky and E. Illés, *Colloid Polym. Sci.*, 2001, **279**, 484–492.
146 E. Tombácz, Z. Libor, E. Illés, A. Majzik and E. Klumpp, *Org. Geochem.*, 2004, **35**, 257–267.
147 D. Kleshchanok, V. Meester, C. E. Pompe, J. Hilhorst and H. N. W. Lekkerkerker, *J. Phys. Chem. B*, 2012, **116**, 9532–9539.
148 J. Landman, E. Paineau, P. Davidson, I. Bihannic, L. J. Michot, A.-M. Philippe, A. V. Petukhov and H. N. W. Lekkerkerker, *J. Phys. Chem. B*, 2014, **118**, 4913–4919.
149 C. K. Abrahamsson, L. Nordstierna, J. Bergenholtz, A. Altskar and M. Nyden, *Soft Matter*, 2014, **10**, 4403–4412.
150 F. Cousin, V. Cabuil and P. Levitz, *Langmuir*, 2002, **18**, 1466–1473.
151 F. L. O. Paula, G. J. da Silva, R. Aquino, J. Depeyrot, J. O. Fossum, K. D. Knudsen, G. Helgesen and F. A. Tourinho, *Braz. J. Phys.*, 2009, **39**, 163–170.

152 F. Van Der Kooij, H. N. L. Lekkerkerker and E. S. Boek, Process fluid, EP 1414926B1, 2004.
153 A. Neaman and A. Singer, *Clays Clay Miner.*, 2000, **48**, 713–715.
154 J. Abdo and M. D. Haneef, *Appl. Clay Sci.*, 2013, **86**, 76–82.
155 Y. C. Chemeda, G. E. Christidis, N. M. T. Khan, E. Koutsopoulou, V. Hatzistamou and V. C. Kelessidis, *Appl. Clay Sci.*, 2014, **90**, 165–174.
156 G. Lagaly, O. Mecking and D. Penner, *Colloid Polym. Sci.*, 2001, **279**, 1090–1096.
157 W. T. Reichle, *Solid State Ionics*, 1986, **22**, 135–141.
158 J. L. Burba and A. L. Barnes, Mixed metal layered hydroxide-clay adducts as thickeners for water and other hydrophylic fluids, US 4,664,843, 1987.
159 J. L. Burba, W. E. Holman and C. R. Crabb, *SPE 17198, SPE/IADC Drilling Conference*, Dallas, Texas, 1988.
160 C. R. Crabb, J. L. Burba and W. E. Holman, *SPE 18482, SPE International Symposium on Oilfield Chemistry*, Houston, Texas, 1989.
161 A. Gilmour and N. Hore, in *AADE ATF 1999*, Houston, Texas, 1999.
162 P. Lange and J. Planck, *Eur. Oil Gas Mag.*, 1999, **25**, 40.
163 G. Lagaly, O. Mecking and D. Penner, *Colloid Polym. Sci.*, 2001, **279**, 1097–1103.
164 H. Wan-Guo, S. De-Jun, H. Shu-Hua, Z. Chun-Guang and W. Guo-Ting, *Colloid Polym. Sci.*, 1998, **276**, 274–277.
165 S. P. Li, W. G. Hou, D. J. Sun, P. Z. Guo, C. X. Jia and J. F. Hu, *Langmuir*, 2003, **19**, 3172–3177.
166 S. P. Li, W. G. Hou, J. C. Xiao, J. F. Hu and D. Q. Li, *Colloids Surf., A*, 2003, **224**, 149–156.
167 S. P. Li and K. Liu, *Colloids Surf., A*, 2007, **304**, 14–17.
168 B. Baruah, M. Mishra, C. R. Bhattacharjee, M. C. Nihalani, S. K. Mishra, S. D. Baruah, P. Phukan and R. L. Goswamee, *Appl. Clay Sci.*, 2013, **80–81**, 169–175.
169 P. Lange, G. Keilhofer and J. Plank, Method for the rheology control of fluid phases, US 6,475,959, 2002.
170 T. B. Hur, T. X. Phuoc, M. K. Chyu and V. Romanov, *Polymer*, 2011, **52**, 2238–2243.
171 P. Lange and J. Plank, *Erdoel ErdGas Kohle (EKEP)*, 1999, **115**, 349–353.
172 R. K. Pujala, N. Pawar and H. B. Bohidar, *Langmuir*, 2011, **27**, 5193–5203.
173 R. K. Pujala and H. B. Bohidar, *Soft Matter*, 2012, **8**, 6120–6127.
174 T. Nakato, Y. Yamashita and K. Kuroda, *Thin Solid Films*, 2006, **495**, 24–28.
175 T. Nakato, Y. Yamashita, E. Mouri and K. Kuroda, *Soft Matter*, 2014, **10**, 3161–3165.
176 H. N. W. Lekkerkerker and R. Tuinier, *Colloids and the depletion interaction*, Springer, Dordrecht, NLD, 2011.

